The Spectrum of Power from Wind Turbines

Jay Apt

***Abstract*—The power spectral density of the output of wind turbines can provide information on the character of fluctuations in turbine output. Here both one second and one hour samples are used to estimate the power spectrum of several wind farms. The measured output power follows a Kolmogorov spectrum over more than four orders of magnitude, from 30 seconds to 2.6 days. The spectrum constrains the character of fill-in power which must be provided to compensate for wind's fluctuations when wind is deployed at large scale. Installing enough linear ramp rate generation to fill in fast fluctuations with amplitudes of 1% of the maximum fluctuation would oversize the fill-in generation capacity by a factor of two for slower fluctuations. A more efficient solution is feasible.**

***Index Terms*—wind, wind energy, wind power generation, spectral analysis.**

I. Introduction

Wind power produced by turbines varies with time. Data with one second time resolution for one 1.5 MW nameplate capacity turbine are shown in Fig. 1. The variability is not dramatically reduced when hourly samples of the output of several turbines in a wind farm are summed, as in Fig. 2, nor when hourly data from four wind farms are summed, as in Fig. 3 (the median hourly change is reduced by 25%).

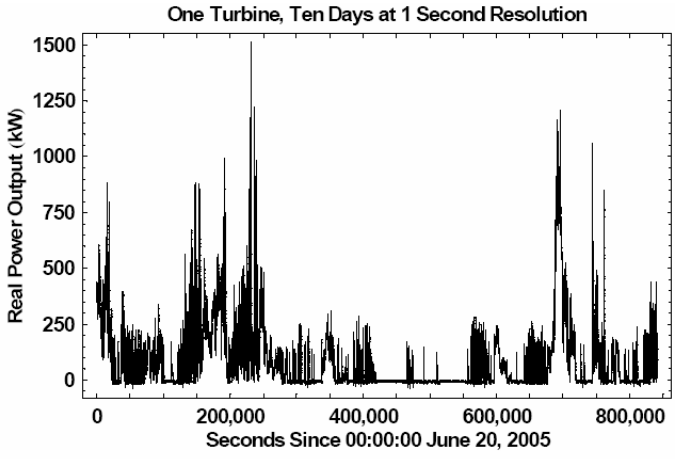

Fig. 1. Real power output (kW) sampled with one second resolution for one 1.5 MW turbine at one wind farm (farm A) for 10 days. Negative values are due to turbine electrical loads.

This work was supported in part by the Alfred P. Sloan Foundation and the Electric Power Research Institute under grants to the Carnegie Mellon Electricity Industry Center, and in part by the U.S. National Science Foundation under awards CCR-0325892, SES-034578, and CNS-0428404.

J. Apt is with the Department of Engineering and Public Policy and the Tepper School of Business, Carnegie Mellon University, Pittsburgh, PA 15213 USA (phone: 412-268-3003; e-mail: apt@cmu.edu).

The output of such turbines is not random. The character of the variations can be examined in several ways. One method [1] is to construct a histogram of the step size in output over time. Here I extend an approach which has seen use over only a limited frequency range [2]: constructing the power spectrum of wind. Data here cover four decades of frequency, using both one second and one hour time resolution data. This frequency range is 100 times larger than that of previous studies.

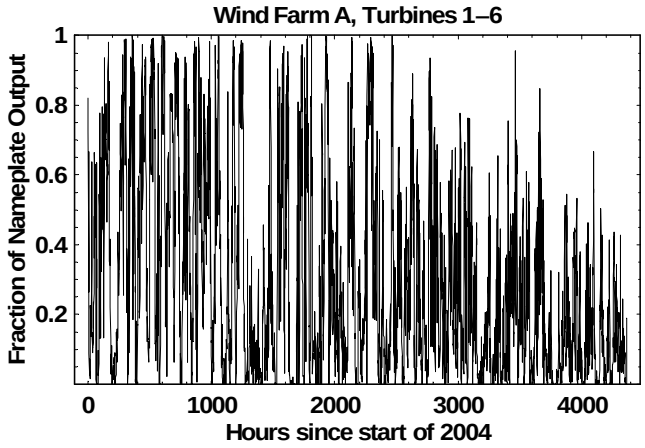

Fig. 2. Real power output as a percent of nameplate capacity sampled with one hour resolution for the sum of the six turbines at wind farm A for the period January 1 – June 30, 2004.

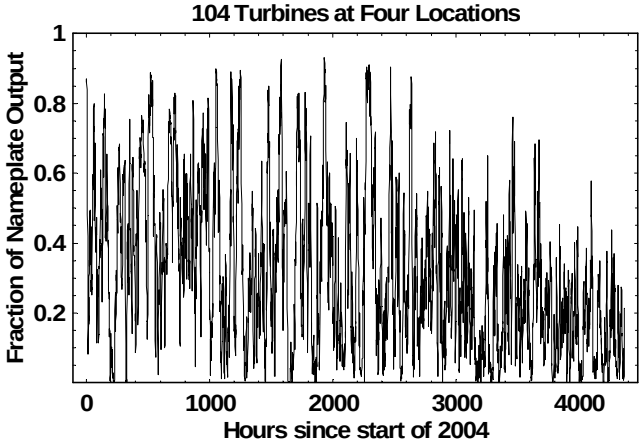

Fig. 3. Real power output as a percent of nameplate capacity sampled with one hour resolution for the sum of the 104 turbines at wind farms A, B, C, and D from January 1 – June 30, 2004.

II. Data

Hourly sampled real power output data with 1 kW power resolution for four wind farms were obtained for the period from 2001 through 2004. The operator of the wind farms has requested that they not be identified by location. The

minimum distance between the generation facilities was 30 km; the maximum was 400 km (Table I). These data were provided for the output of each wind farm, not for individual turbines. For certain periods, the data were supplied with 1 MW power resolution. All four locations had 1 kW resolution hourly data available for the period January 1 through June 30, 2004. Wind farms A and B had 1 kW hourly data for July 1, 2003 through June 30, 2004.

TABLE I
DISTANCE (KM) BETWEEN WIND FARMS

	A	B	C
D	320	350	400
A		30	100
B			90

One second sampled real power output data with 0.1 watt power resolution for each of the six turbines at wind farm A and each of the ten turbines at wind farm B were obtained for a ten-day period in 2005. Wind farm A data for the final day ceased after approximately the first 21 hours, leaving a total of 841,600 continuous samples (Fig. 1). Wind Farm B data were good throughout, giving a total of 864,000 continuous samples. The individual turbine outputs were then summed to give the output of each wind farm (Fig. 4 and Fig. 5).

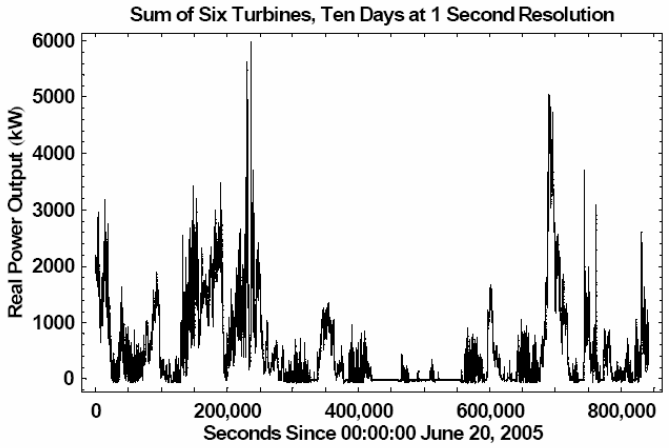

Fig. 4. Real power output (kW) at one second resolution as the sum of the six turbines at wind farm A over a ten-day period.

III. GEOGRAPHIC CORRELATION

The 4368 hourly data points from January – June 2004 were used to examine the correlation of the power output between each pair of wind farms. Pearson's correlation coefficient,

$$\sum_i (x_i - \bar{x})(y_i - \bar{y}) \Big/ \left(\sqrt{\sum_i (x_i - \bar{x})^2} \sqrt{\sum_i (y_i - \bar{y})^2} \right) \quad (1)$$

was used to determine the linear correlation between the real power outputs of the facility pairs. More detailed techniques are available for other correlation analysis [3].

The output power of wind farms which are in relatively close proximity are strongly positively correlated (Table II).

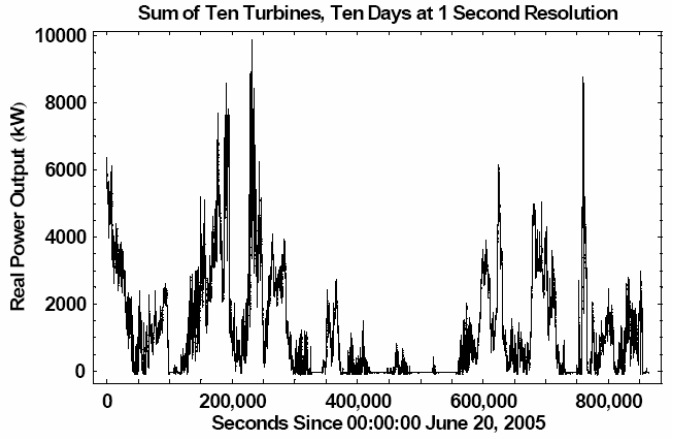

Fig. 5. Real power output (kW) at one second resolution as the sum of the ten turbines at wind farm B over a ten-day period.

The highest observed correlation was between wind farms B and C. Each point in Fig. 6 is the real power output from one hour in the data set for these two facilities.

TABLE II
OUTPUT POWER CORRELATION BETWEEN WIND FARMS,
JANUARY 1 – JUNE 30, 2004

	A	B	C
D	0.46	0.35	0.36
A		0.69	0.71
B			0.77

Even at a distance of 400 km, there is a fair degree of positive correlation between wind farm D and the other three facilities.

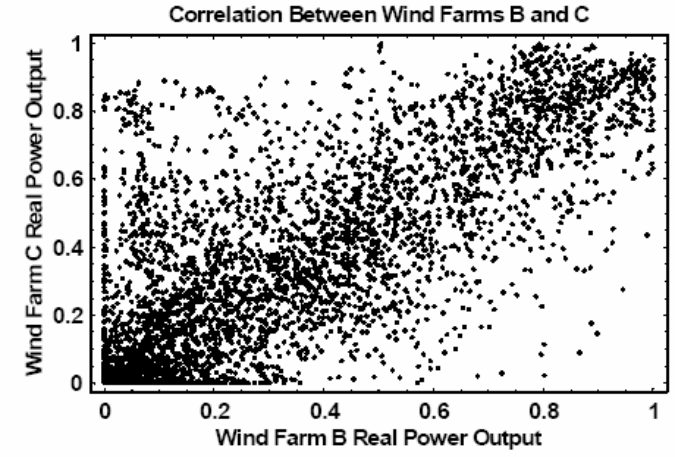

Fig. 6. Real power output as a fraction of nameplate capacity of wind farms B and C for the first 4368 hours of 2004. Each point represents one hourly datum.

IV. SPECTRAL ANALYSIS PROCESSING

To estimate the power spectrum (sometimes termed the power spectral density or PSD) of the real power output of a wind farm, we first compute the discrete Fourier transform of the time series of output measurements. We use an N-point-

long equal interval time sample of the output c(t) to construct the value at frequency domain point k, C_k [4]

$$C_k = \sum_{j=0}^{N-1} c_j e^{2\pi i j k/N} \qquad k = 0, 1, \ldots, N-1 \qquad (2)$$

The periodogram estimate of the power spectrum at frequency domain point k is then [5]

$$P_0 = \frac{1}{N^2} \left| C_0^2 \right|$$

$$P_{f_k} = \frac{1}{N^2} \left[|C_k^2| + |C_{N-k}^2| \right] \quad k = 1, 2, \ldots, \frac{N}{2} - 1 \qquad (3)$$

$$P_{f_{max}} = \frac{1}{N^2} \left| C_{N/2}^2 \right|$$

where the relationship between the frequency and frequency domain point k is given by

$$f_k = 2 f_{max} \frac{k}{N} \qquad k = 0, 1, \ldots, \frac{N}{2} \qquad (4)$$

and f_{max} is (in concert with the Nyquist sampling theorem) 0.5 Hz for the one second data, and 1.4 x 10^{-4} Hz for the one hour data.

The periodogram is normalized so that the sum of all points P is the mean squared amplitude of the time series c(t). To enable better comparison with other attributes of the electric power system, the graphs which follow display the square root of the periodogram, so that the units are in kW/$\sqrt{\text{Hz}}$.

One of the attributes of power spectrum estimation through periodograms is that increasing the number of time samples (N) does not decrease the standard deviation of the periodogram at any given frequency f_k. In order to take advantage of a large number of data points in a data set to reduce the variance at f_k, the data set may be partitioned into several time segments. The Fourier transform of each segment is then taken and a periodogram estimate constructed. The periodograms are then averaged at each frequency, reducing the variance of the final estimate by the number of segments (and reducing the standard deviation by the reciprocal of the square root of the number of segments).

In this work, eight segments are used. This has no effect on f_{max}, but increases the lowest non-zero frequency (f_1) by a factor equal to the number of segments. Thus, the 366 days of hourly data treated in this manner have a minimum frequency component of 2.5 x 10^{-7} Hz and a maximum frequency corresponding to two hours (1.4 x 10^{-4} Hz). When this technique is used, the ten-day time series acquired at one second resolution has frequency components from a minimum of 9.2 x 10^{-6} Hz to a maximum of 0.5 Hz

Data windowing with both a Bartlett and Welch window followed by segment overlapping by one-half the segment length [6] was tried on the one-second resolution data, with no noticeable improvement in the variance. The power spectra presented below were estimated without windowing (i.e. using a square window) and without overlapping the segments. In order to ensure that the processing introduced no artifacts in the power spectra, the wind farm A 1 second data were replaced by pseudorandom data (generated using a Marsaglia-Zaman subtract-with-borrow algorithm [7]) with the same maximum and minimum as the wind farm A data. The resulting PSD was flat on a log-log plot, as expected for random data.

V. Power Spectra

Using the method discussed in the previous section, the power spectra for the wind farms A and B were estimated, using hourly sampled data from July 1, 2003 – June 30, 2004 and using 1-second sample data from a 10-day period.

The spectrum of the output of the sum of the six turbines at wind farm A using the hourly sampled data (Fig. 7) and the one-second interval data (Fig. 8) were combined to yield a spectrum from 2 seconds to 6 weeks (Fig. 9).

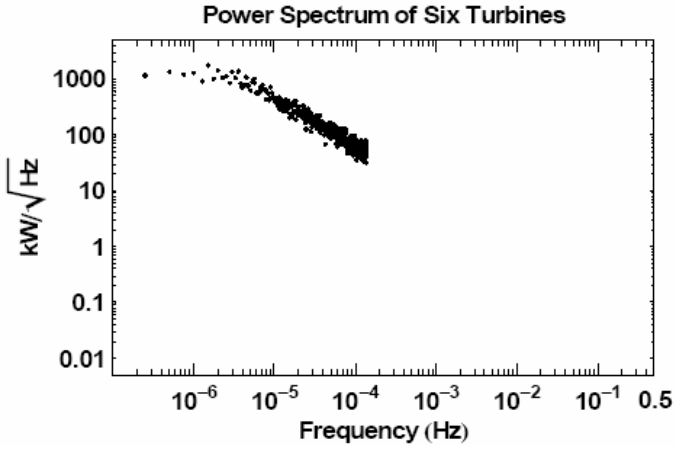

Fig. 7. Power spectrum of data sampled at one hour resolution of the sum of the six at wind farm A from July 1, 2003 – June 30, 2004 using 8-segment averaging.

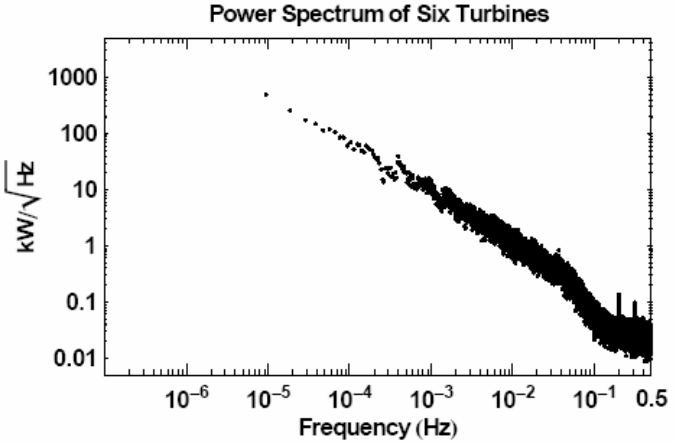

Fig. 8. Power spectrum of data sampled at one second resolution of the sum of the six 1.5 MW turbines at wind farm A using 8-segment averaging.

The spectrum of the output of the sum of the ten wind farm B turbines using the hourly sampled data and the one-second interval data are combined in Fig. 10.

The combined spectra of Figs. 9 and 10 are characterized by four different regions. At frequencies between 2 x 10^{-6} and 4 x 10^{-2} Hz, the double logarithm plot of the spectrum is linear (i.e. exponential in frequency). At frequencies above ~5 x 10^{-2} Hz, the physical and electrical inertia of the turbines

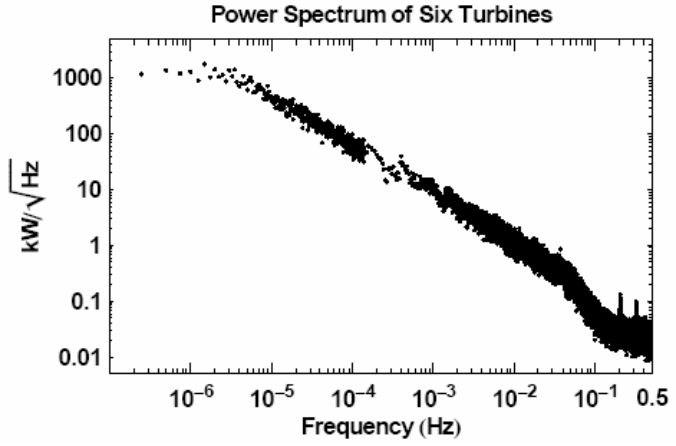

Fig. 9. Combined wind farm A power spectra from Fig. 7 and Fig. 8.

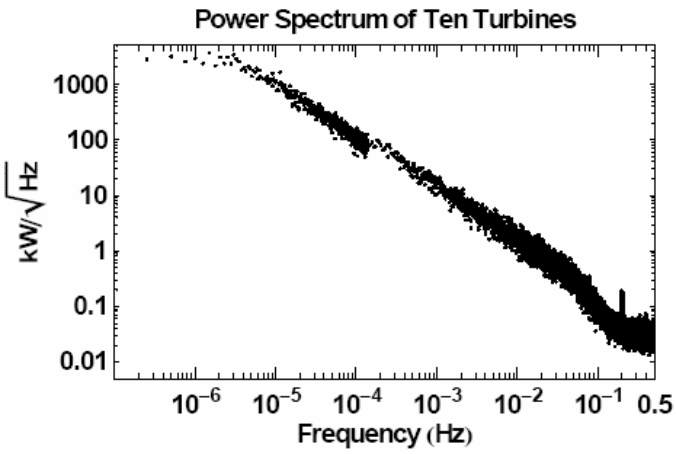

Fig. 10. Combined power spectrum of data sampled at one hour and one second resolution of the sum of the ten turbines at wind farm B using 8-segment averaging.

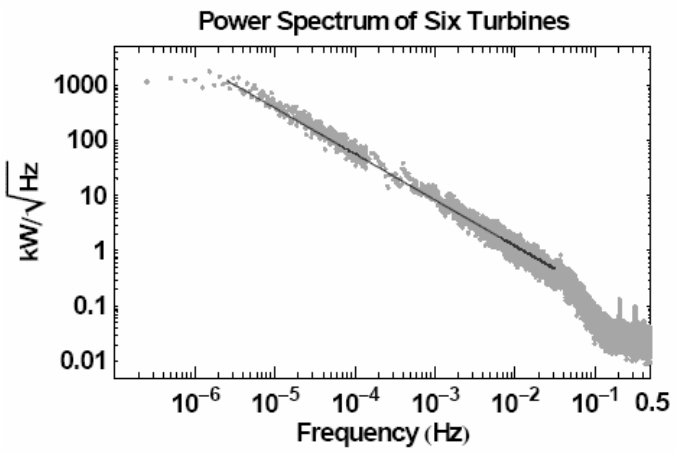

Fig. 11. The combined wind farm A spectra of Fig. 9 (grey points) and a $f^{-5/3}$ spectrum (solid line).

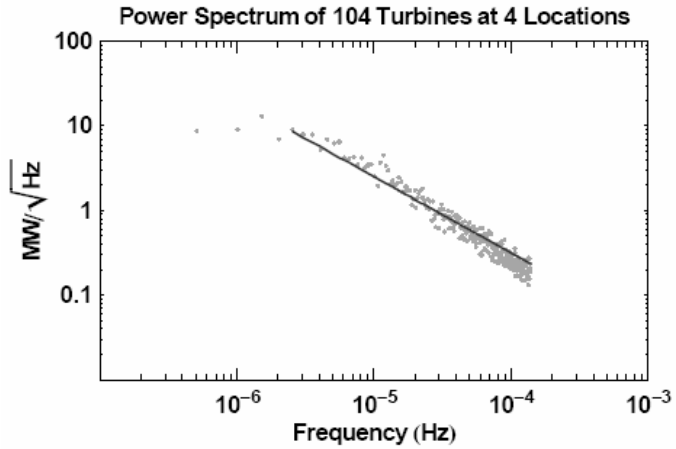

Fig. 12. The hourly spectra of the combined output of all four wind farms shown in Fig. 3 (grey points) and a $f^{-5/3}$ spectrum (solid line). Note the scale change on the ordinate from previous figures.

appear to act as low-pass filters. Frequencies between 10^{-1} and 5×10^{-1} Hz show the noise floor of the output power sensors. Peaks in the spectrum in this region are generally due to the turbine blade passing frequencies [8]. At frequencies below roughly 2×10^{-6} Hz the maximum output of the turbines provides an upper limit to the spectrum.

The linear region of the power spectrum plot is well fit by an exponential function in frequency of the form $f^{-5/3}$ (Fig. 11).

The combined output of all four wind farms also follows the same form, over the frequency range sampled by the hourly data (Fig. 12).

VI. Kolmogorov Spectrum

The Reynolds number (ratio of inertial to viscous force) of the Earth's atmosphere can be ~ 10^6. For sufficiently large Reynolds number, viscous effects can be neglected, and the energy dissipation in wind is dependent on only inertial forces. In this regime, for an incompressible fluid, Kolmogorov's second hypothesis of similarity [9] predicts that the power spectrum should vary as $f^{-5/3}$.

The first experimental verification of Kolmogorov's spectrum was in an ocean tidal channel near Vancouver, over two decades of frequency [10]. Similar spectra have been observed in the atmosphere [11].

Previous published power spectra of wind generator power [2] have linear regions of the power spectrum plot covering one or two decades of frequency. These studies have not provided a comparison between their data and the Kolmogorov spectrum.

A power spectrum of wind speed from 1.9×10^{-7} to 0.25 Hz published in 1957 [12] has been reprinted in a recent handbook [13] and review paper [14]. This spectrum has a pronounced "spectral gap" between about 3×10^{-5} and 7×10^{-3} Hz with very little energy. The data analyzed here show no such gap, and an area-preserving plot (frequency times PSD against the log of frequency) shows a smooth behavior through this region. This disagreement may arise from the way in which the older spectra were measured (at several different altitudes) or in the way those data from several time periods were combined.

The measured output power in this study follows a Kolmogorov spectrum over more than four orders of magnitude in frequency, from 30 seconds to 2.6 days. The actual atmospheric behavior may extend further, since these data are constrained by the turbine inertia at high frequencies and by the maximum output of the turbines at low frequencies.

VII. Implications of the Kolmogorov Spectrum

Output power of individual turbines or wind farms can effectively be modeled by a $f^{-5/3}$ relation for a broad range of frequencies, extending from the turbine inertial limit at high frequency to the wind farm power output limit at low frequency.

Modeling of wind power systems has used the Kolmogorov spectrum for flicker analysis at frequencies above 10^{-2} Hz [8]. Caution should be used at frequencies above roughly 5 x 10^{-2} Hz for turbines such as those measured here, because their inertia has the effect of applying a low pass filter to the wind spectrum (Figs. 9 – 12).

Wind at small scale is sometimes treated by grid operators as negative load. To examine the validity of this empirical practice, load data from a control area near the turbines used in this study were obtained with 14 second resolution for the first 180 days of 2004. The PSD (Fig. 13) estimated in the same way as for the wind power data above shows the expected peaks at 1 day and its harmonics, as well as the weekly peak. There is a region, between 1 hour and 2.5 minutes, in which the spectrum of this region's load is fit well by a Kolmogorov spectrum. In this interval, the practice of treating wind power fluctuations as negative load appears to be justified. Note that this is not the same thing as saying that load fluctuations cancel wind fluctuations, as is sometimes stated, since the two would have to be both of the same magnitude and anti-correlated for the assertion to be valid.

Since wind is an intermittent resource, it must be matched with fill-in power sources from storage or generation if the power output of wind farms on a grid are correlated.

If wind at very large scale were to be used, what ramp rate characteristics would be required by the fill-in energy? The ensemble of generators, energy storage, and demand response used should have a power spectrum which matches that of the wind generators.

A line connecting the 24 hour load peak and its harmonics (Fig. 13) falls off roughly as $f^{-7/2}$. This rapid decrease in power at high frequency allows the use of slow-ramping generators to match the fluctuations. However, the $f^{-5/3}$ curve for wind power means that high frequency fluctuations contain considerable power.

A linear ramp rate generator is not the optimum match for wind. The power spectral density for such a generator has the form f^{-2}. Suppose that such a generator were to be sized to compensate for the variations in wind power at 1 percent of the maximum variations observed. This point is reached at roughly 2.5 x 10^{-4} Hz for the systems shown in Figs 9 and 10. Then (because the slope of the generator's PSD is steeper than the Kolmogorov spectrum) the generator would be sized to compensate for fluctuations about twice as large as the maximum actually observed at low frequencies.

A more efficient match between wind's fluctuations and fill-in power can be made by noting that the source is required to match fluctuations at high frequency, but at much reduced amplitude compared to the match required at low frequency.

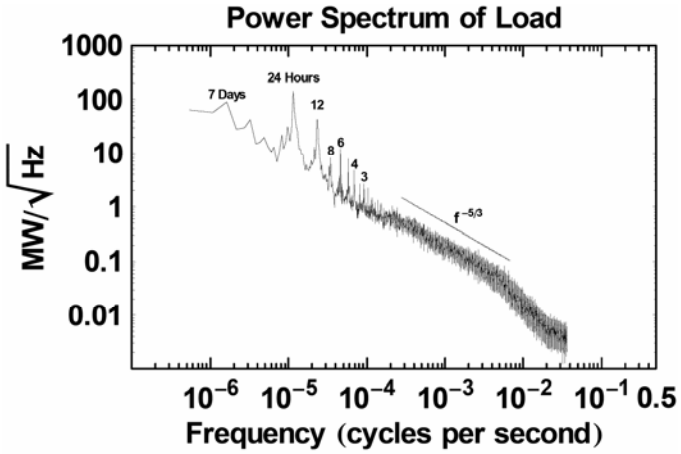

Fig. 13. The spectrum of load in one control area near the turbines used for this study for 180 days at 14-second time resolution using 8-segment averaging, and a Kolmogorov spectrum ($f^{-5/3}$) displaced upwards from the best fit amplitude for clarity.

Rather than size a linear ramp rate generator to match fluctuations in the output power of wind farms, a more efficient solution is to match wind with an ensemble of generators, energy storage, and demand response. Fast devices or demand response with relatively low power would match the short-period fluctuations, while slower ramp rate sources would match the longer period, higher amplitude fluctuations. Further work will quantify the economically optimum mix, but the capital savings from not over-building linear ramp rate matching generation by a factor of two can be large for wind at large scale.

Acknowledgment

The author thanks Joseph DeCarolis, M. Granger Morgan and José Moura for helpful discussions.

References

[1] See for example, Wan, Y. (2004). "Wind power plant behaviors: analyses of long-term wind power data." National Renewables Energy Laboratory technical report NREL/TP-500-36551., available: http://www.nrel.gov/docs/ fy04osti/36551.pdf; and Wan, Y. and D. Bucaneg (2002). "Short-term power fluctuations of large wind power plants". *J. Solar Energy Engineering* 124(4): 427-431.

[2] Sørensen, P. A.D. Hansen, P. Andre, and C. Rosas (2002). "Wind models for simulation of power fluctuations from wind farms". *J. Wind Eng. Ind. Aerodyn.* 90(12-15): 1381-1402.; McNerney, G. and R. Richardson (1992). "The statistical smoothing of power delivered to utilities by multiple wind turbines". *IEEE Trans. Energy Conv.* 7(4): 644-647; and Thiringer, T. (1996). "Power quality measurements performed on a low-voltage grid equipped with two wind turbines". *IEEE Trans. Energy Conv.* 11(3): 601-606.

[3] Sørensen, P. *et al*. (2002). *Op cit.*

[4] Bracewell, R. (1965). *The Fourier Transform and Its Applications,* McGraw-Hill.

[5] Press, W.H., S.A. Teukolsky, W.T. Vetterling, and B.P. Flannery (1992). *Numerical Recipes in FORTRAN: The Art of Scientific Computing,* Cambridge University Press, p. 544.

[6] *ibid.*, p. 549.

[7] Marsaglia, G. and A. Zaman (1991). "A new class of random number generators". Ann. Appl. Probability 1(3): 462-480.

[8] Moreno, C.V., H.A. Duarte, and J.U. Garcia (2002). "Propagation of flicker in Electric Power Networks due to wind energy conversion systems". *IEEE Trans. Energy Conv.*17(2): 267-272.

[9] Kolmogorov, A. N. (1941). "The local structure of turbulence in incompressible viscous fluids at very large Reynolds numbers". *Dokl. Akad. Nauk. SSSR*, 30: 301–305. Reprinted (1991) *R. Soc. Lond. Proceedings: Mathematical and Physical Sciences*, 434 (1890): 9-13.

[10] Grant, H. L., R. W. Stewart and A. Moilliet (1961). "Turbulence spectra from a tidal channel". *J. Fluid Mech.*, 12: 241–263.

[11] Monin, A.S. (1967). "Turbulence in the Atmospheric Boundary Layer". *Physics of Fluids,* 10 (9P2): S31-S37, and Kaimal, J.C. (1973). "Turbulence spectra, length scales, and structure parameters in the stable surface layer". *Boundary Layer Meteorology*, 4: 289-309.

[12] Van der Hoven, I. (1957). "Power spectrum of horizontal wind speed in the frequency range from 0.0007 to 900 cycles per hour". *J. Meteorology*, 14: 160-164.

[13] Burton, T., D. Sharpe, N. Jenkins, and E. Bossanyi (2001). *Wind Energy Handbook*, chapter 2, John Wiley & Sons, Chichester.

[14] Fordham, E.J. (1985). "The spatial structure of turbulence in the atmospheric boundary layer". *Wind Eng.* 9: 95-133.